

Efficiency in nanostructured thermionic and thermoelectric devices

M. F. O'Dwyer,* R. A. Lewis, and C. Zhang

*School of Engineering Physics and Institute for Superconducting and Electronic Materials,
University of Wollongong, Wollongong NSW 2522, Australia*

T. E. Humphrey

*School of Physics, University of New South Wales, Sydney NSW 2052, Australia
Baskin School of Engineering, University of California Santa Cruz, Santa Cruz, CA 95064-1077*

(Dated: March 23, 2022)

Advances in solid-state device design now allow the spectrum of transmitted electrons in thermionic and thermoelectric devices to be engineered in ways that were not previously possible. Here we show that the shape of the electron energy spectrum in these devices has a significant impact on their performance. We distinguish between traditional thermionic devices where electron momentum is filtered in the direction of transport only and a second type, in which the electron filtering occurs according to total electron momentum. Such ‘total momentum filtered’ k_F thermionic devices could potentially be implemented in, for example, quantum dot superlattices. It is shown that whilst total momentum filtered thermionic devices may achieve efficiency equal to the Carnot value, traditional thermionic devices are limited to efficiency below this. Our second main result is that the electronic efficiency of a device is not only improved by reducing the width of the transmission filter as has previously been shown, but also strongly depends on whether the transmission probability rises sharply from zero to full transmission. The benefit of increasing efficiency through a sharply rising transmission probability is that it can be achieved without sacrificing device power, in contrast to the use of a narrow transmission filter which can greatly reduce power. We show that devices which have a sharply-rising transmission probability significantly outperform those which do not and it is shown such transmission probabilities may be achieved with practical single and multibarrier devices. Finally, we comment on the implications of the effect the shape of the electron energy spectrum on the efficiency of thermoelectric devices.

PACS numbers: 73.23.Ad, 73.63.-b, 73.15.Jf, 79.40.+z

I. INTRODUCTION

Traditional vacuum thermionic power generators [1, 2, 3] with macroscopic gaps between emitter and collector plates are limited to very high temperature applications ($T_H > 1000$ K). Refrigeration using such devices, as first suggested by Mahan [4], is also limited to high temperatures due to a lack of suitable materials with work-functions below ~ 0.3 eV.

Nanostructures are currently being investigated in an attempt to develop thermionic devices that can refrigerate or generate power at lower temperatures. The potential for achieving lower barrier heights via the use of semiconductor heterostructures was pointed out by Shakouri and Bowers [5, 6], with Mahan et al. [7, 8] suggesting multilayers as a means of reducing the phonon heat leaks inherent in the use of solid-state rather than vacuum devices. Successful solid-state thermionic cooling of up to a few degrees has been reported [9, 10, 11, 12].

Another promising direction is the use of nanometer gaps between the emitter and the collector to lower the work function via quantum tunnelling [13, 14], with Hishinuma et al. reporting cooling of about a mK in such a system. Cooling by field emission from carbon nanotubes and other nanostructures has also been proposed [15, 16].

In thermoelectrics, nanostructured devices may offer the possibility of substantially increasing the thermoelectric fig-

ure of merit, ZT , over that of traditional bulk bismuth telluride based devices ($ZT \approx 1$) due to enhanced electron transport and phonon blocking properties. Hicks and Dresselhaus have predicted that ZT can be enhanced using quantum-well superlattices [17] and quantum wires [18]. Venkatasubramanian et al. have reported the highest ZT to date, $ZT \sim 2.4$ using a p-type $\text{Bi}_2\text{Te}_3/\text{Sb}_2\text{Te}_3$ superlattice [19]. Other methods used and suggested for the enhancement of the figure of merit include the use of quantum-dot superlattices [20, 21], superlattices with a non-conservation of lateral momentum [22, 23], inhomogeneous doping [24] and nanotubes [25].

Many of these approaches offer the possibility of engineering the energy spectrum (the number of electrons transmitted through the device as a function of energy) in a way that was not possible in traditional vacuum thermionics or bulk thermoelectrics. In light of the new design freedom offered by nanostructures, it is useful to re-examine the impact of the electron energy spectrum upon what has been called the ‘electronic efficiency’ of thermionic devices [26], defined as the efficiency associated with strictly electronic processes under ideal conditions of particle transport.

Improvements in electronic efficiency due to better device design which can be achieved without lowering the power will translate into an improvement in the operating efficiency of practical thermionic devices where non-ideal effects, such as phonon and radiative leaks, as well as contact and lead resistances, are important. To achieve high overall efficiency in practical devices it is important to design devices that not only achieve low thermal conductivity, but high electronic efficiency at finite power as well.

*Electronic address: mo15@uow.edu.au

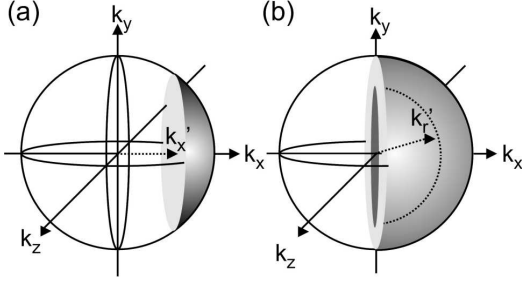


FIG. 1: Fermi spheres indicating electrons transmitted by (a) a k_x filtered device and (b) a k_r filtered device.

In this paper we analyse in detail the dependence of the electronic efficiency of thermionic power generators and refrigerators upon the details of the energy spectrum of electrons transmitted ballistically between the emitter and collector. The term energy filtering is often used to indicate a restriction of electron flux to all those electrons above a certain energy. Here the term energy filtering will be used in a more general sense to indicate any arbitrary restriction on the energy spectrum of transmitted electrons. We examine two idealised models of thermionic nanodevices. In the first, energy (or more precisely, momentum) filtering of electrons occurs in the direction of transport only. This model, which we will denote as a ' k_x -filtered thermionic device', is applicable to single-barrier or multibarrier (superlattice) solid-state devices. In the second model, which we will denote as a ' k_r -filtered thermionic device', energy filtering of the total energy of electrons is assumed to be possible. This model is applicable to vacuum emission from nanostructures such as carbon nanotubes and solid-state devices in which there is periodic modulation of the potential in all three dimensions (such as quantum dot superlattices), or superlattices in which there is non-conservation of electron momentum in directions perpendicular to transport [22, 23]. Fig. 1 shows geometrically the range of electrons transmitted in idealised k_x and k_r type devices in momentum space.

With thermoelectric devices, the presence of a bandgap in different crystallographic directions ensures electrons contributing to the current have a certain minimum value of momentum in all three dimensions. The close relationship between thermionic and thermoelectric devices has been analysed by a number of authors [8, 27, 28, 29]. In this paper, this comparison is extended to similarities between the dependence of the electronic efficiencies of these devices on the details of the electron energy spectrum.

Three main results are presented in this paper. Firstly, it is shown that while k_r devices may achieve electronic efficiency equal to the Carnot value, conventional k_x devices are fundamentally limited to efficiencies less than this. Secondly, the details of the electron energy spectrum are shown to have a significant impact on the electronic efficiency of the device. Narrower electron energy filters and, more significantly, a sharp rise in the transmission probability from zero to complete transmission give dramatic improvements in electronic efficiency. Using a numerical model of ballistic trans-

port in semiconductor hetrostructures, we show that sharply rising transmission probabilities yielding high electronic efficiency and power may be achieved with wide single barrier and multibarrier devices. Finally, the equivalence of the ballistic and diffusive formalisms for devices with length the order of the electron mean free path [29] means that in this regime, the electronic efficiency of thermionic and thermoelectric devices will have the same dependence upon the details of the electron energy spectrum.

II. TRANSPORT THEORY

A. Ballistic Transport Theory

A thermionic device consists of two electron reservoirs at different temperatures and electrochemical potentials, separated by a barrier, or series of barriers, which limit the flow of electrons between them to a certain energy range. Whether the device operates as a power generator, pumping high-energy electrons from the hot to the cold against the electrical potential difference, or as a refrigerator, removing high-energy electrons from the cold reservoir, depends upon the relative magnitudes of the opposing temperature and electrochemical potentials.

In a k_r -filtered thermionic device, where the transmission probability, ζ , is a function of the total electron energy, $E = \hbar^2 \mathbf{k}^2 / 2m^*$, the net electrical current density flowing from the cold to the hot reservoir is

$$J_r = q \int_0^\infty [n_r^C - n_r^H] \zeta(E) dE \quad (1)$$

where $q = -1.602 \times 10^{-19}$ C is the charge of an electron and

$$n_r^{C/H} = \frac{m^* E}{2\pi^2 \hbar^3} f(E, \mu_{C/H}, T_{C/H}) \quad (2)$$

is the number of electrons with total energy E arriving at the three-dimensional reservoir interface per unit area per unit time and

$$f(E, \mu_{C/H}, T_{C/H}) = \left[1 + \exp \left(\frac{E - \mu_{C/H}}{k_B T_{C/H}} \right) \right]^{-1} \quad (3)$$

is the Fermi-Dirac distribution function in the cold/hot reservoir with chemical potential $\mu_{C/H}$ and temperature $T_{C/H}$. We have assumed that electron velocity is determined by the reservoirs. A more detailed theory would be required to account for any velocity changes due to the device structure.

One may calculate the heat flux out of the hot and cold reservoirs by noting that an electron leaving or entering the cold/hot reservoir will remove or add respectively an amount of heat equal to the difference between the energy of the electron and the average energy of electrons in the reservoir, that is $E - \mu_{C/H}$. Introducing this factor inside the integral for number current we may obtain expressions for the net heat flux out of the cold/hot reservoir as

$$\dot{Q}_r^{C/H} = \mp \int_0^\infty (E - \mu_{C/H}) [n_r^C - n_r^H] \zeta(E) dE. \quad (4)$$

In a k_x -filtered device the transmission probability is a function of what may be loosely defined as the ‘kinetic energy of electrons in the x direction’, $E_x = \hbar^2 k_x^2 / 2m^*$. It is therefore convenient in this case to write the electrical and heat currents in terms of E_x [30]

$$J_x = q \int_0^\infty [n_x^C - n_x^H] \zeta(E_x) dE \quad (5)$$

where

$$n_x^{C/H} = \frac{m^* k_B T_{C/H}}{2\pi^2 \hbar^3} \log \left[1 + \exp \left(-\frac{E_x - \mu_{C/H}}{k_B T_{C/H}} \right) \right] \quad (6)$$

is the number of electrons with kinetic energy in the x direction E_x arriving at the reservoir interface per unit area per unit time.

In a k_x -filtered device, the average heat removed from the cold/hot reservoir when an electron with energy in the x direction E_x leaves, $E_x + k_B T_{C/H} - \mu_{C/H}$ (assuming Maxwell-Boltzmann statistics), is not the same as that added when an electron with energy in the x direction E_x arrives, $E_x + k_B T_{H/C} - \mu_{C/H}$. This difference is due to the fact that, while the barrier system filters electrons according to their momentum in the direction of transport, their momenta in the other two dimensions may take any value, contributing on average an extra $k_B T_{C/H}$ to the energy of electrons emitted from the cold/hot reservoir. The heat flux out of the cold/hot reservoir in a k_x filtered device is therefore given by

$$\dot{Q}_x^{C/H} = \mp \int_0^\infty [(E_x + k_B T_{C/H} - \mu_{C/H}) n_x^C - (E_x + k_B T_{H/C} - \mu_{C/H}) n_x^H] \zeta(E_x) dE. \quad (7)$$

It may be noted that many cryogenic ballistic refrigerators such as normal-insulating-semiconductor (NIS) junction devices [31, 32, 33] and quantum dot refrigerators [34] utilise either two- or one-dimensional reservoirs where the difference between k_x and k_r filtered devices are less dramatic or non-existent.

The electronic efficiency as a power generator and coefficient of performance (COP) as a refrigerator for both k_x and k_r filtered devices are given by

$$\eta^{PG} = VJ / \dot{Q}^H \quad (8)$$

and

$$\eta^R = \dot{Q}^C / VJ \quad (9)$$

respectively, where $V = (\mu_C - \mu_H) / q$.

B. Diffusive Transport Theory

Thermoelectric devices are generally differentiated from thermionic devices according to whether electron transport is diffusive or ballistic [8]. There is, however, little to distinguish the underlying thermodynamics of the two types of device, with both achieving reversibility under the same conditions [24, 35] and both being governed by the same ‘materials parameter’ [28, 29, 36].

Under the relaxation-time approximation the electric current in a thermoelectric device may be calculated using the Boltzmann transport equation as

$$J^d = \iiint q D_l [v_x^d]^2 \tau \frac{df}{dx} d\mathbf{k}. \quad (10)$$

where D_l is the local density of states (DOS), $\tau = \tau_0 E^r$ is the relaxation time, and $v_x^d = (1/\hbar)[\partial E(k_x)/\partial k_x]$ is the velocity in the direction of transport. The electron energy spectrum in a diffusive device is thus determined by $D_l [v_x^d]^2 \tau [df/dx]$.

The transport equation for ballistic devices, where the mean free path of an electron between collisions is greater than the width of the barrier, or system of barriers, may be written similarly as

$$J^b = \iiint q D_r \zeta v_x^r \Delta f d\mathbf{k} \quad (11)$$

where $D_r = 1/(2\pi)^d$ is the DOS in k -space in the reservoirs where d is the dimensionality of the reservoirs, and $\Delta f = f_C - f_H$ is the difference between the distribution functions in the cold and hot reservoirs. The electron energy spectrum in a thermionic device is therefore determined by $D_r v_x^r \zeta \Delta f$.

We expect that Eqs. 11 and 10 should yield the same results for devices of width close to the electron mean free path. If we take the energy dependence of the relaxation time to be $r = -1/2$, which is appropriate when scattering is dominated by acoustic phonons, the mean free path in the direction of transport will be independent of energy and given by $\lambda \equiv v_x \tau$ [29]. For a small piece of thermoelectric material of length approximately equal to the electron mean free path $df/dx \approx \Delta f / \lambda$. Eq. 10 then reduces to [29]

$$J^d = \iiint q D_l v_x^d \Delta f d\mathbf{k} \quad (12)$$

and is of the same form as that of the ballistic transport equation, Eq. 11. Thus, the term $D_l v_x^d$ in the diffusive formalism plays the same role as $D_r v_x^r \zeta$ in the ballistic formalism. We therefore expect the dependencies of the electron energy spectrum in both thermionic and thermoelectric device to be similar. Since v_x^r and D_r are fixed by the reservoirs, at fixed temperature/chemical potential the electron energy spectrum in a ballistic device is determined by the transmission probability as device structure varies. In a diffusive device, both D_l and v_x^d may change when the device structure is altered and affect the energy spectrum.

The heat-current density out of the cold/hot reservoir is given by

$$\dot{Q}_{C/H} = \mp \iiint (E - \mu_{C/H}) D_l v_x^d \tau \frac{df}{dx} d\mathbf{k}. \quad (13)$$

Due to the equivalence of the diffusive and ballistic formalisms in this regime, the intensive efficiency across a small section of thermoelectric material [37, 38] and the electronic efficiency/COP of a ballistic device are given by Eqs. 8 and 9 respectively.

III. REVERSIBLE ELECTRON TRANSPORT

To achieve reversibility in a thermionic or thermoelectric device, electrons must flow only at energies where the Fermi occupation of states, Eq. 3, is constant [24, 35]. Assuming a finite temperature difference at each end of the device, there are two different quasi-static limits in which this requirement is satisfied.

The first way is to restrict the flow of electrons to those with energies approaching infinity where the occupation of states tends to zero. This may be achieved, for instance, with an intrinsic semiconductor where the band gap approaches infinity in a thermoelectric device or an infinitely high barrier system in a thermionic device. In vacuum thermionic devices operating at very high temperatures ($T_H > 1500$ K), optimum efficiency is approached when the barrier height is almost 20 times larger than $k_B T_H$ [26], meaning that electronic efficiencies close to the Carnot limit may be obtained. However, at the more moderate emitter temperatures, $300 \text{ K} < T_H < 800 \text{ K}$, of interest in most applications, achieving finite power production or refrigeration via a thermionic device requires a much lower barrier height, of the order of a few $k_B T_H$. It is therefore more practical to utilize the other quasi-static limit to achieve high electronic efficiencies.

The second way to achieve reversibility in a thermionic or thermoelectric device, which we refer to as energy-specific equilibrium, is to allow electrons to flow only at a single energy where the Fermi occupation of states throughout the device is the same [35],

$$E_0 = \frac{\mu(T + \delta T) - (\mu - \delta\mu)T}{\delta T} \quad (14)$$

where δT and $\delta\mu$ are the temperature and chemical potential changes respectively over a distance δx in the device. At this energy, the effect, or, in the language of irreversible thermodynamics, the ‘affinity’ [39], of the opposing temperature and electrochemical potential gradients upon electrons exactly cancels and transport occurs reversibly. This is also the energy at which the energy-resolved current changes sign, that is, for electrons with energies less than E_0 the net current flows from the hot to cold reservoir and for energies greater than E_0 net current flows from the cold to hot reservoir. Transport of electrons of a single energy only might be achieved using resonant tunneling in a superlattice or quantum dot superlattice. For a thermionic device, the ballistic transmission energy is determined substituting the cold and hot reservoir temperatures and chemical potentials into Eq. 14. Here we shall denote a filtering system which transmits only a single energy of electrons between the reservoirs, be that the single total energy for a k_r device or a single x energy for a k_x device, as an ‘ideal filter’. For a ballistic device this may be expressed as a transmission probability function as

$$\zeta(E) = \begin{cases} 1 & E = E' \\ 0 & \text{elsewhere} \end{cases} \quad (15)$$

where E_x would be substituted for E in a k_x system.

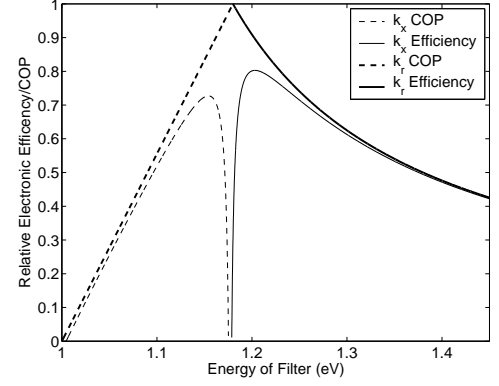


FIG. 2: Relative efficiency and COP of ideally filtered k_r and k_x devices versus the energy of the ideal filter. The k_x curves are plotted against the total average energy of electrons leaving the cold reservoir, $E_x + k_B T_C$. $T_H = 300 \text{ K}$, $T_C = 270 \text{ K}$, $\mu_H = 0.98 \text{ eV}$ and $\mu_C = 1.00 \text{ eV}$.

In a thermoelectric device, inhomogeneous doping or a graded band structure is required so that Eq. 14 may be satisfied at every point in the device for a particular temperature gradient such that the energy gap between the chemical potential and the transmission energy is given by [24]

$$E_0 - \mu_0(x) = \left[\frac{eV_{OC}}{T_H - T_C} \right] T(x) \quad (16)$$

where V_{OC} is the open circuit voltage.

IV. ELECTRONIC EFFICIENCY WITH IDEAL FILTERING

Under ideal filtering, as defined in the previous section, Eqs. 8 and 9 for the k_r device reduce to

$$\eta_r^{PG} = \frac{\mu_C - \mu_H}{E_0 - \mu_C} \quad (17)$$

for power generation ($E' > E_0$) and

$$\eta_r^R = \frac{E_0 - \mu_C}{\mu_C - \mu_H} \quad (18)$$

for refrigeration ($E' < E_0$). The efficiency and COP of ideally filtered k_x and k_r systems are plotted in Fig. 2 relative to the Carnot values. When the filtering energy is E_0 , reversibility and the Carnot efficiency are achieved for the k_r device as shown in Fig. 2. The energy axis for the k_x device shown in Fig. 2 is the average total cold reservoir energy, $E_x + k_B T_C$.

For all values of total energy shown in Fig. 2, the k_r device outperforms the k_x device. Importantly, unlike the k_r device, the k_x filtered thermionic device does not reach the Carnot efficiency for arbitrary electrochemical potentials and finite barrier heights. The reason for this is that although momentum in the x direction is restricted to a single value, the momentum in the y and z directions may take any value, meaning

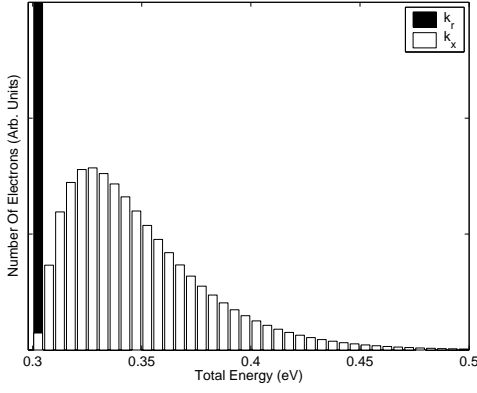


FIG. 3: The total energy distributions for electrons leaving a reservoir in k_x and k_r filtered thermionic devices with a filter of 5 meV at 0.3 eV. The vertical axis has been cut off for clarity of the details in the k_x system values. The number of electrons transmitted in the k_r system is approximately 13 times that of the k_x system for these parameters. $T = 270$ K and $\mu = 0.1$ eV.

that the energy spectrum has a finite width and reversibility is not achieved. The distributed nature of total electron energies for a k_x device, even with a narrow filter, is shown in Fig. 3. For k_x -filtered power generators, this upper bound upon the electronic efficiency can be obtained analytically in the limit that $(\mu_C - \mu_H)/k_B(T_H - T_C) \gg 1$, in which case maximum efficiency is obtained when $E' = E_0$, where

$$\eta_x^{PG} = \eta_C [1 + \eta_C(k_B T_H + k_B T_C)/qV]^{-1} \quad (19)$$

where η_C is the Carnot efficiency. Given that we have taken $\mu_C > \mu_H$, so that qV is positive, it can be seen by inspection that Eq. 19 always yields an efficiency less than η_C . For the system analysed in Fig. 2, Eq. 19 gives a maximum electronic efficiency for the k_x power generator of 80% of the Carnot limit, in agreement with numerical results. This constitutes the first main result of the paper, that for finite barrier heights and electrochemical potential differences, k_x filtered thermionic devices are limited to a maximum electronic efficiency less than the Carnot limit. This means that from the point of view of maximising electronic efficiency, k_r devices are inherently superior to k_x devices.

V. ELECTRONIC EFFICIENCY WITH NON-IDEAL FILTERING

The filters considered in Sect. IV represent an idealized theoretical limit. We now extend our analysis to non-ideal filters. Firstly, we consider filters of finite width where all electrons over a certain range of total or x energies are transmitted. Secondly, we show that a gradual, rather than sharp switch from zero to full transmission has a significant impact on the electronic efficiency of thermionic devices. This will constitute the second main result of the paper.

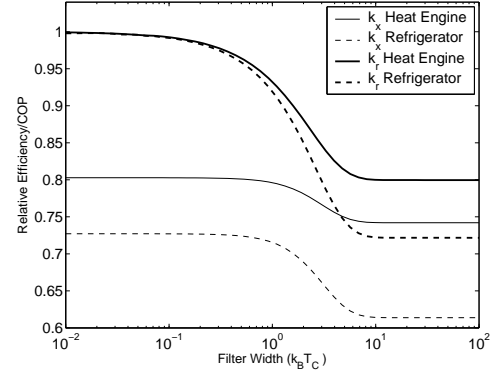


FIG. 4: The maximum relative efficiency and COP as a fraction of the Carnot limit for k_r and k_x filtered thermionic devices versus the width of the filter from $0.01k_B T_C$ to $100k_B T_C$. $T_H = 300$ K, $T_C = 270$ K, $\mu_H = 0.98$ eV and $\mu_C = 1.00$ eV.

A. Effect of Finite Filter Width

A filter of finite width corresponds to a transmission probability of

$$\zeta(E) = \begin{cases} 1 & E' < E < E' + \Delta E \\ 0 & \text{elsewhere} \end{cases} \quad (20)$$

for a k_r system, and where E_x would be substituted for E for a k_x system. Such a filter might be used, for example, to approximate a transmission miniband in a superlattice device. For each filter width examined numerically, the starting energy of the filter, E' , was tuned to find the maximum electronic efficiency/COP for that width. The results for filters of width $0.01k_B T_C$ to $100k_B T_C$ are plotted in Fig. 4. The filter of $0.1k_B T_C$ is narrow enough to effectively perform ideal filtering, reflected in the fact that the k_r electronic efficiency/COP approaches the the Carnot value for this width and the k_x values reach the maximum values obtained in Fig. 2. Fig. 4 shows however that we do not require an ideal filter to achieve an efficiency/COP very close to the maximum value, as seen in the plateau in all curves. The k_r and k_x systems may achieve an efficiency/COP approximately equal to the maximum value for filter widths of less than about $0.1k_B T_C$ and $k_B T_C$ respectively. Filter widths of around these sizes are achievable using practical semiconductor devices as will be discussed later. As the filter widths increase beyond these values the efficiency/COP drops and then plateaus again at a final value. Large filter widths effectively correspond to the situation where all electrons above E' are being transmitted. As the distribution function rapidly converges to zero at high energies, this means that further increasing filter width has a minimal effect upon the electronic efficiency.

Fig. 5 shows the energy spectrum of the net electric current transmitted from the hot to cold reservoir for a 0.3 eV wide filter. Results are normalized by the net number of electrons with total energy greater than the Fermi energy available to flow between reservoirs such that the number of electrons in

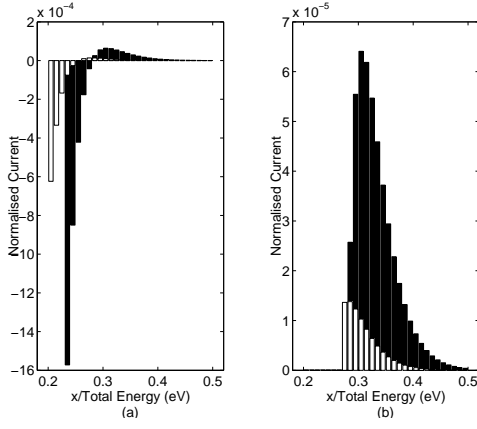


FIG. 5: The normalised electron energy spectrum for net current from the hot to cold reservoir. The filter width is 0.3 eV and is positioned to achieve maximum efficiency/COP in each system for (a) refrigeration and (b) power generation in k_r (black) and k_x (white) systems. $T_C = 270$ K, $T_H = 300$ K, and $\mu_C = 0.1$ eV, $\mu_H = 0.08$ eV.

i th energy band are given by

$$N_i = \frac{\int_{E_i}^{E_i+\delta i} n_{r/x} dE}{|\int_{\mu_C}^{\infty} n_r dE|}. \quad (21)$$

It should be noted that the k_x energy spectrum in Fig. 5 does not show the total energy spread due to the unfiltered degrees of freedom, as was shown in Fig. 3, since in this case we are considering the spectrum with regard to filtered x component of energy only. This illustrates the energy range of the filter for each system when tuned for maximum electronic efficiency/COP.

Fig. 5 shows that there are more electrons being transmitted for the k_r system than with the k_x system, an effect previously pointed out by Vashae and Shakouri [22, 23], which results in greater power in a k_r device. The calculations presented here show that the difference in the energy spread of electrons in k_x and k_r filtered devices also gives an increase in the electronic efficiency for k_r devices due to a greater concentration of electrons with energies around E_0 . For both refrigeration and power generation, the filters will be positioned such that electrons with energy E_0 are included. Since when $E > E_0$ the net energy-resolved current produces power, the lower edge of the k_r power generator filter will always be at E_0 . For the k_x system this lower edge is shifted to lower x energy due to the additional energy contribution in the two other spatial degrees of freedom. Energy-resolved current in the energy range $\mu_C < E < E_0$ refrigerates the cold reservoir and the lower edge of the filter is therefore shifted to this region in Fig. 5(a). Since there are more electrons at higher energies, however, current flow in the region $E > E_0$ generates power and a trade off occurs when positioning the filter for maximum COP. Again, the x energy of the k_x filter is lower than the total energy of the k_r filter due to the unfiltered energy contributions.

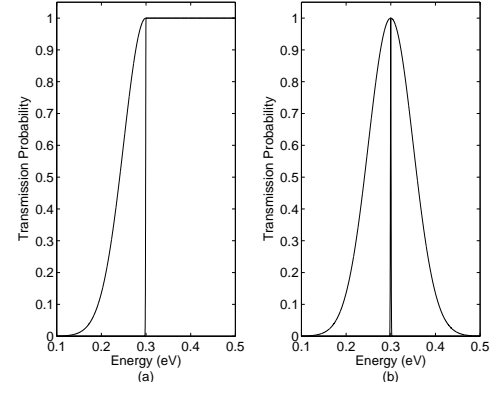


FIG. 6: Artificial transmission probabilities generated using a (a) Gaussian function and (b) a half-Gaussian function. The two extremes of width parameter are shown, $w = 0.1$ (slowly rising) and $w = 0.00001$ (sharply-rising).

B. Transmission Probabilities With Finite Slopes

Thus far we have considered only the case where there is a sharp transition from zero to full transmission of electrons. In this section we consider the effect upon the electronic efficiency of a gradual transition, which more closely resembles the shape of the transmission probability in practical devices. We begin by using two convenient ‘artificial’ transmission probabilities, the slope of which can be easily varied. The first, a Gaussian peak which might approximate the transmission probability of a resonance, is given by

$$\zeta(E) = \exp\left(-\frac{(E - E_c)^2}{w}\right) \quad (22)$$

where E_c defines the center energy of the peak and w is a width parameter which is used to vary the sharpness of the slope. E_x would be substituted for E for a k_x device.

The second artificial transmission probability considered is a ‘half-Gaussian’ intended to approximate the transmission probability of a single barrier of finite width. This is given by Eq. 22 for $E \leq E_c$ and is equal to one for $E > E_c$. The sharpness of the Gaussian and half-Gaussian transmission probabilities were varied between $w = 10^{-5}$, corresponding to an ideal filter or perfectly sharp single barrier transmission probability, and $w = 0.1$. The transmission probabilities associated with these extreme values are shown in 6(a) and (b). The system bias was tuned for each transmission probability for maximum electronic efficiency/COP. Fig. 7(a) shows the COPs associated with a room temperature refrigerator and Fig. 7(b) shows the electronic efficiencies of a heat engine operating at higher temperature.

Since all electrons of energy other than E_0 reduce the electronic efficiency we expect the sharpest peak in Figs. 7(a) and (b) to yield the highest efficiency/COP, and this is confirmed by the numerical results. The most interesting result, however, is that the electronic efficiency of the half-Gaussian transmission probability is very strongly dependent upon how sharply the transmission rises from zero to unity. A smooth rise in

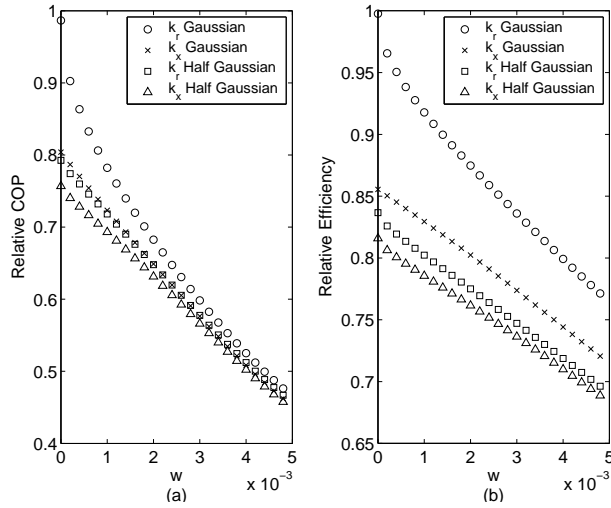


FIG. 7: The efficiency/COP relative to the Carnot value of a k_r Gaussian, k_x Gaussian, k_r half-Gaussian and k_x half-Gaussian for (a) refrigerator systems ($T_H = 300$ K and $T_C = 270$ K) and (b) heat engine systems ($T_H = 900$ K and $T_C = 300$ K) versus width parameter with $\mu_C = 0.1$ eV.

the transmission probability lowers the electronic efficiency for the same physical reason that a k_x filtered device has a lower electronic efficiency than a k_r filtered device. Net current flow is from the hot to cold reservoir for electron energies just above E_0 , generating power with efficiency approaching the Carnot limit. Conversely, net current flow is from the cold to the hot reservoir for electron energies below E_0 and above μ_C , absorbing power and refrigerating the cold reservoir, while the net current transmitted at energies below μ_C both absorb power and heat the cold reservoir. This means that whenever the energy spectrum of transmitted electrons rises slowly to its peak value there is an efficiency lowering trade off which occurs between transmitting the maximum number of electrons with energies near E_0 , which refrigerate or generate power with Carnot efficiency, and minimising the number of electrons transmitted in the range $E < E_0$ for power generation or in the range $E < \mu_C$ and $E > E_0$ for refrigeration. As the transmission probabilities become less sharp, the performance difference between the k_x and k_r and Gaussian and half-Gaussian systems becomes less significant.

So far we have established the two criteria for maximum electronic efficiency in thermionic power generators and refrigerators. Firstly, we have shown that the narrower the energy spectrum the higher the electronic efficiency. However, in general a gain in electronic efficiency via this mechanism is obtained at the expense of the power of the device. The second criterion is that the sharper the transition from zero to peak value in the energy spectrum, the higher the electronic efficiency. This second method offers the significant advantage of improving the electronic efficiency without sacrificing power through the use of a narrow filter. The maximum power achievable is also greater with a sharply-rising transmission probability if the barrier height is optimised [40]. In the next section we analyse design considerations for thermionic de-

vices considering both electronic efficiency and power.

VI. DESIGN CONSIDERATIONS FOR ACHIEVING HIGH ELECTRONIC EFFICIENCY IN PRACTICAL DEVICES

A. Ballistic Devices

Semiconductor-based devices, including superlattices, may be specifically designed to achieve the desired energy spectrum features in k_x devices. Filter widths around those required for achieve near-maximum electronic efficiency, as discussed in Sect.V A, may be achieved using a variably-spaced superlattice energy filter (VSSEF) as proposed by Summers, Brennan and Gaylord [41, 42]. Such devices consist of alternating semiconductor layers with barrier and well widths chosen such that energy levels in the wells are closely aligned under bias. Tunneling through a simpler multibarrier structure may also suffice. Similarly, a miniband in the transmission probability for a superlattice might be used as a narrower filter compared with complete transmission above the barrier energy. Quantum dot structures [43] or normal-insulating-superconductor junction (NIS) devices [34] can also achieve narrow electron transmission bands and may be used for refrigeration at cryogenic temperatures. Relatively narrow energy electron emission peaks from carbon nanotubes have been reported which may be of use in a vacuum based device [44]. Since the DOS in the reservoirs fixes the number of electrons available for transport in a certain energy range in ballistic devices, the reduction of power in narrow transmission probability devices, with only modest gains in electronic efficiency, is expected to be undesirable in the presence phonon heat leaks.

It is likely that the best way to simultaneously achieve high electronic efficiency and high power in a ballistic device is to design the structure such that the transmission probability rises sharply from zero to one and remains close to unity beyond this. Whilst the most obvious way to achieve a transmission probability of this nature is to utilise a single barrier with a width as large possible (but less than the mean free path of electrons) here we show that an array of thin barriers can also be used to engineer a transmission probability that rises sharply from zero to unity.

The transmission probabilities and associated efficiencies/COPs for single rounded barriers of various widths have been calculated. The transmission probabilities were calculated by obtaining a numerical solution to the time-independent Schrödinger equation based on Airy functions [30, 45]. Fig. 8 shows the significant difference in sharpness between a 10-nm and 100-nm barrier. We see in Fig. 9, as expected, the wider barriers with sharper transmission probabilities give the highest efficiencies/COPs approaching the maximum value, in this case, at a width of around 35 nm. Beyond this width, there is little to be gained in terms of electronic efficiency, although phonon mediated heat leaks continue to be reduced with increasing barrier width.

From another point of view, wide barriers might be undesirable. Devices with greater interface density may reduce

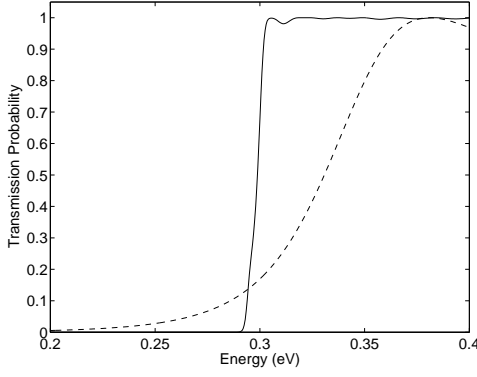


FIG. 8: The transmission probability of a 10-nm (dashed line) and 100-nm (solid line) rounded single 0.3-eV barrier systems under no applied bias. Effective mass is $0.067m_e$.

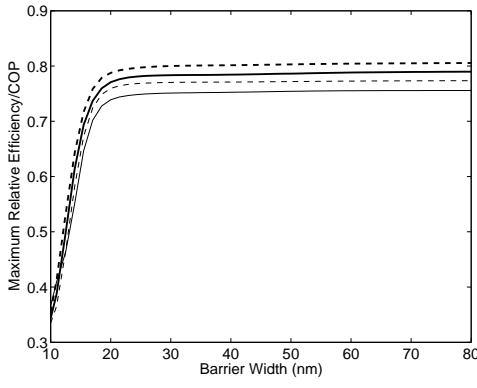


FIG. 9: The relative electronic efficiency and COP of single barrier k_r heat engine (thick-dashed line), k_x refrigerator (thick-solid line), k_x heat engine (thin-dashed line) and k_x refrigerator (thin-solid line) devices versus the width of the barrier. $T_C = 270$ K, $T_H = 300$ K, $\mu_C = 0.1$ eV, barrier height of 0.3 eV and effective mass of $0.067m_e$.

thermal conductivity as a result of interface scattering and phonon miniband formation [46]. Here we consider a device where multiple barriers are traversed in an electron mean free path. This allows quantum mechanical effects to be utilised to achieve high electronic efficiency using narrow barriers which give low electronic efficiency when used individually.

Multiple narrow barriers over a distance of the order of the electron mean free path may be used to give a transmission probability that is as sharp as if the electrons were traversing a single wide barrier. Figs. 10(a) and (b) show the transmission probabilities calculated for two-barrier and eight-barrier systems respectively as well as the very smoothly rising transmission probability for a single 5-nm barrier for comparison. The efficiencies/COPs achieved are within 3% of those of a wide single barrier. Thus, high electronic efficiencies may be achieved, whilst allowing the flexible use of narrower barriers.

The ‘turn-on’ transmission energy for a device with many thin barriers may be shifted to lower energy as shown in Fig. 11(a) and (b). If the chemical potential remains constant, this lowering of the turn-on energy may result in a decrease in

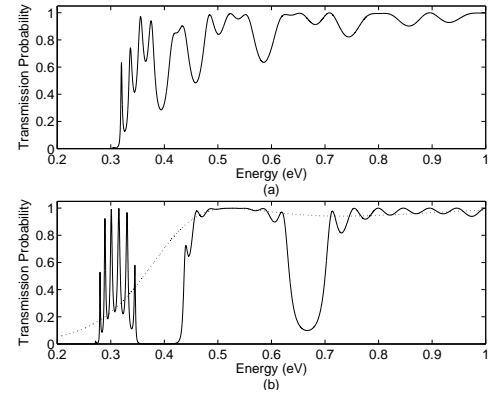


FIG. 10: Transmission probabilities calculated for (a) a two 20-nm barrier system with 20-nm well and (b) an eight 5-nm barrier system with 5-nm wells (solid) and the transmission probability for a single 5-nm barrier (dotted) for comparison. $T_C = 270$ K, $T_H = 300$ K, $\mu_C = 0.1$ eV, barrier height of 0.3 eV and effective mass of $0.067m_e$.

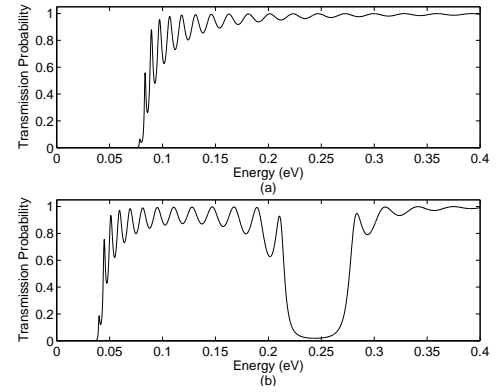


FIG. 11: Transmission probabilities calculated for: (a) An 80-nm single barrier with maximum k_x refrigerator COP of 0.59 when $\mu_C = 0$ eV and 0.48 when $\mu_C = 0$ eV, (b) A 15 3-nm barrier system with 3-nm wells with k_x refrigerator COPs of 0.48 when $\mu_C = 0$ eV. $T_C = 270$ K, $T_H = 300$ K, barrier height of 0.075 eV and effective mass of $0.05m_e$.

efficiency and increase in power compared to a wider single barrier due to the decrease in the work function, $\phi = E_{turnon} - \mu$. With the same work functions, which may be achieved by altering the chemical potentials as detailed in Figs. 11(a) and (b), the wide single barrier and many thin barrier systems achieve approximately the same electronic efficiency.

We do not expect a dramatic change in dependence of device behaviour on the electron energy spectrum as the total length of the device increases beyond an electron mean free path. Since the probability of an electron traveling distance L without suffering a collision is given by [47]

$$P = \exp(-\lambda/L) \quad (23)$$

the ballistic and diffusive formalisms, Eqs. 11 and 10, may be combined to show that the electrical current will be given

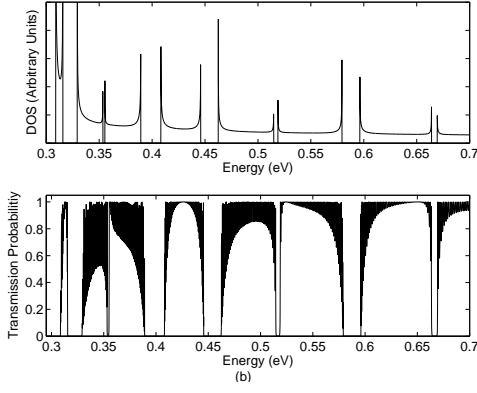


FIG. 12: (a) The local DOS for an infinite series of 20-nm barriers separated by 20 nm and (b) the transmission probability for fifty 20-nm barriers separated by 20 nm with a barrier height of 0.3 eV and effective mass of $0.067m_e$.

by [29]

$$J = \iiint q \Delta f \left(D_r v_x^r \zeta P + \frac{\lambda}{L} D_l v_x^l [1 - P] \right) d\mathbf{k} \quad (24)$$

if $L \approx \lambda$. As the number of barriers increases and the overall length of the device becomes significantly greater than the electron mean free path, the ballistic term becomes small so that transport is accurately described using the diffusive formalism, as discussed in the next section.

B. Diffusive Devices

As was discussed earlier, the energy spectrum in a diffusive device is determined by the product of the local DOS, the velocity squared and the relaxation time at constant temperatures/chemical potentials. The local DOS of an infinite superlattice may be determined using the Kronig-Penney model [30, 48]. Fig. 12 shows the DOS calculated for a many-barrier system and the calculated transmission probability showing the clear relationship between the two. In a pure ballistic device, since the DOS and velocity are fixed by the reservoirs, a sharp electron energy spectrum is achieved via a sharp transmission probability. In diffusive devices, both the DOS and electron velocity may change as the device structure changes and it may be a difficult optimisation problem to design a structure where their product changes sharply from its minimum to maximum value as a function of energy [49].

Mahan and Sofo have shown that the ideal transport distribution function for a thermoelectric device may be achieved with a delta function DOS [50]. Humphrey and Linke showed that the Carnot efficiency may be achieved in thermoelectric devices utilising a delta function DOS and a graded device structure or inhomogeneous doping [24]. Their results are analogous to the results presented earlier in this paper where it was shown that the ideal transmission probability for a ballistic device was one which allowed the transmission of only a very narrow energy range of electrons. The results presented in this paper suggest that not only is the width of the energy

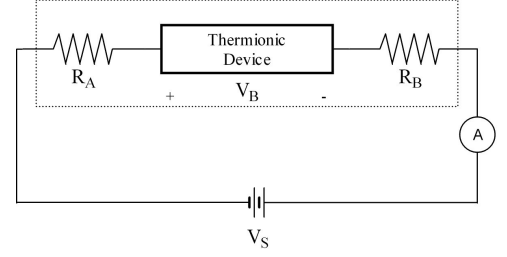


FIG. 13: A thermionic circuit showing contact resistances R_A and R_B , source voltage V_S and barrier voltage V_B .

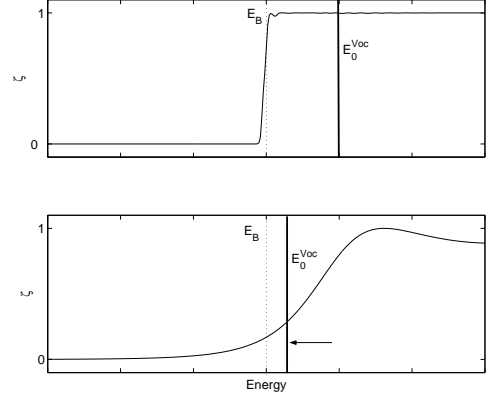


FIG. 14: The transmission probabilities for (a) a wide and (b) a narrow single barrier. E_0^{Voc} is indicated by the dashed line and the barrier energy, E_B by the dotted line.

spectrum important, but also whether it rises rapidly from zero to its maximum value. In practical devices with loss mechanisms such as phonon heat leaks, the magnitude of the energy spectrum also becomes important to the efficiency as the conductivity is given by the integral of the energy spectrum and occupation of states. Hicks and Dresselhaus have pointed out that the magnitude of the DOS can be increased by using structures of lower dimensionality, potentially increasing the power factor [17, 18]. We also note that the DOS is sharper for lower dimensional systems compared to bulk materials, which may result in an improved energy spectrum.

VII. EXPERIMENTALLY OBSERVABLE PROPERTIES RELATED TO ELECTRONIC EFFICIENCY

The presence of phonon heat leaks and contact resistance in solid-state thermionic devices makes direct measurements of the electronic efficiency difficult. Here we discuss experimental properties which may be measured to provide an indication of the shape of the electron energy spectrum and though this, electronic efficiency.

The I-V characteristics of a thermionic device are dependent on the voltage across the barrier system, V_B , as shown on Fig. 13. V_B may be determined from the supplied voltage, V_S ,

and measured current, I , as

$$V^B = V^S + I(R_A + R_B) \quad (25)$$

where, R_A and R_B are contact resistances, when the device is generating power. As the bias is increased, the net electrical current decreases and reaches zero at the open circuit voltage V_{OC}^B , from which the effective Seebeck coefficient may be calculated as

$$S = \frac{V_{OC}^B}{T_H - T_C}. \quad (26)$$

The energy-specific equilibrium energy may be calculated at open circuit voltage as

$$E_0^{V_{OC}} = \mu_C + V_{OC}^B \frac{T_C}{T_H - T_C} = \mu_C + ST_C \quad (27)$$

and is linearly related to the Seebeck coefficient. $E_0^{V_{OC}}$ is the energy where energy-resolved currents above and below it are equal, giving zero net current. For a sharply-rising transmission probability, $E_0^{V_{OC}}$ would be positioned as shown in Fig. 14(a) above the barrier energy. If we have another system where electrons with energies lower than the barrier energy are being transmitted without significant change to the high-energy details, for example through decreasing the barrier width, $E_0^{V_{OC}}$ is shifted to lower energy as shown in Fig. 14(b). Measuring this relative to a convenient energy, say the barrier energy, E_B , provides a convenient sharpness indication for the transmission probability,

$$\psi = ST_C - \phi. \quad (28)$$

The ‘turn-on’ energy for a multibarrier system may be shifted to lower energy, in which case, the sharpness indicator should be measured relative to this ‘effective’ barrier height, which might be calculated using the Kronig-Penney model, as discussed previously. A higher sharpness indicator is desirable, indicating a sharper transmission probability and therefore higher expected electronic efficiency/COP. The sharpness indicator has the advantage over the Seebeck coefficient of being less dependent on the chemical potential/barrier height and more so on the sharpness of the energy spectrum, as shown in Fig. 15. Here, the chemical potentials for a number of single barrier transmission probabilities have been varied to give a constant Seebeck coefficient as the barrier width and transmission probability sharpness change. Fig. 15 shows the electronic efficiency varies significantly in this example. Whilst the Seebeck coefficient remains constant, the sharpness indicator, ψ , increases as the electronic efficiency increases.

VIII. CONCLUSIONS

It has been shown the the nature of the electron-energy spectrum has a significant impact on the performance of thermionic and thermoelectric devices. The limiting efficiency of finite barrier height devices was achieved when electrons of a single energy only are transmitted. Whilst k_r devices

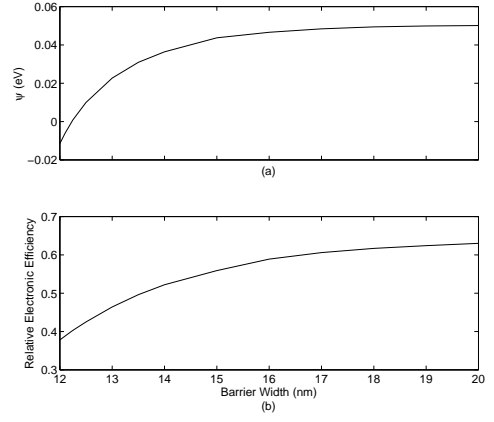


FIG. 15: The (a) maximum relative electronic efficiency and (b) sharpness indicator versus single barrier width. The cold reservoir chemical potential has been tuned so that the Seebeck coefficient is constant for each barrier width. $T_C = 270$ K, $T_H = 300$ K, barrier height of 0.3 eV and effective mass of $0.067m_e$.

achieve reversibility when the transmission energy was equal to E_0 , k_x devices do not due to the finite energy spread associated with the two unfiltered degrees of freedom. For systems with finite-width rectangular transmission probabilities, electronic efficiency was close to the maximum value for filter widths less than $k_B T$, but decreases as the range of transmitted electron energies increases, reaching a steady value as the filter width increases beyond a few $k_B T$. Our most important result was that an increase in the sharpness of the rise in electron energy spectrum significantly increases electronic efficiency. Improving the electronic efficiency by increasing the sharpness of the transmission probability may also increase the maximum power. We have shown that sharp transmission probabilities may be achieved using wide single barriers or carefully arranged multiple barriers.

Since, in the diffusive formalism, used to describe thermoelectric devices, the product of the local electron group velocity and the local DOS plays the same role as the product of the reservoir DOS, reservoir velocity and the transmission probability in the ballistic formalism for mean free path length devices, the results presented here showing the benefit of sharply-rising energy spectra on electronic efficiency and power are expected to be relevant to thermoelectric devices.

Finally, the sharpness indicator, ψ , was suggested as an experimental measure providing an indication of the sharpness of the rise in the energy spectrum of a ballistic device and its electronic efficiency and was shown to be superior for this purpose to the Seebeck coefficient alone.

IX. ACKNOWLEDGEMENTS

MO'D is supported by the Australian Research Council. TH is supported by the Australian Research Council and funding from ONR MURI. The authors acknowledge helpful discussions with Ali Shakouri and Heiner Linke.

-
- [1] W. Schlichter, Ph.D. thesis, University of Gottingen (1915).
- [2] V. C. Wilson, J. Appl. Phys. **30**, 475 (1959).
- [3] J. M. Houston, J. Appl. Phys. **30**, 481 (1959).
- [4] G. D. Mahan, J. Appl. Phys. **76**, 4362 (1994).
- [5] A. Shakouri and J. E. Bowers, 16th Annual Conference on Thermoelectrics pp. 636–340 (1997).
- [6] A. Shakouri and J. E. Bowers, Appl. Phys. Lett. **71**, 1234 (1997).
- [7] G. D. Mahan and L. M. Woods, Phys. Rev. Lett. **80**, 4016 (1998).
- [8] G. D. Mahan, J. O. Sofo, and M. Bartkowiak, J. Appl. Phys. **83**, 4683 (1998).
- [9] A. Shakouri, C. LaBounty, J. Piprek, P. Abraham, and J. E. Bowers, Appl. Phys. Lett. **74**, 88 (1999).
- [10] C. Labounty, A. Shakouri, P. Abraham, and J. E. Bowers, Proceedings of SPIE **3950**, 69 (2000).
- [11] X. Fan, G. Zeng, E. Croke, C. LaBounty, D. Vashaee, A. Shakouri, and J. Bowers, Electronics Letters **37**, 126 (2001).
- [12] X. Fan, E. Croke, C. A. Ahn, S. Huxtable, A. Majumdar, and A. Shakouri, Appl. Phys. Lett. **78**, 1580 (2001).
- [13] Y. Hishinuma, T. H. Geballe, B. Y. Mozyhes, and T. W. Kenny, Appl. Phys. Lett. **78**, 2572 (2001).
- [14] Y. Hishinuma, B. Y. Mozyhes, T. H. Geballe, and T. W. Kenny, Appl. Phys. Lett. **81**, 4242 (2002).
- [15] N. M. Miskovsky and P. H. Cutler, Appl. Phys. Lett. **75**, 2147 (1999).
- [16] T. S. Fisher and D. G. Walker, Journal of Heat Transfer **124**, 954 (2002).
- [17] L. D. Hicks and M. S. Dresselhaus, Phys. Rev. B **47**, 12727 (1993).
- [18] L. D. Hicks and M. S. Dresselhaus, Phys. Rev. B **47**, 16631 (1993).
- [19] R. Venkatasubramanian, E. Siivola, T. Colpittes, and B. O’Quinn, Nature **413**, 597 (2001).
- [20] T. C. Harman, P. J. Taylor, M. P. Walsh, and B. E. LaForge, Science **297**, 2229 (2002).
- [21] A. A. Balandin, Appl. Phys. Lett. **82**, 415 (2003).
- [22] D. Vashaee and A. Shakouri, J. Appl. Phys. **95**, 1233 (2004).
- [23] D. Vashaee and A. Shakouri, Phys. Rev. Lett. **92**, 106103 (2004).
- [24] T. E. Humphrey and H. Linke, Phys. Rev. Lett. **94**, 096601 (2005).
- [25] X. B. Zhao, X. H. Ji, Y. H. Zhang, J. P. Tu, and X. B. Zhang, Appl. Phys. Lett. **86**, 06211 (2005).
- [26] G. N. Hatsopoulos and E. P. Syftopoulos, *Thermionic Energy Conversion Volume I: Processes and Devices* (The MIT Press, London, 1973).
- [27] G. S. Nolas and H. J. Goldsmid, J. Appl. Phys. **85**, 8 (1999).
- [28] C. B. Vining and G. D. Mahan, J. Appl. Phys. **86**, 6852 (1999).
- [29] T. E. Humphrey, M. F. O’Dwyer, C. Zhang, and R. A. Lewis, J. Appl. Phys. (In Press).
- [30] J. H. Davies, *The Physics of Low Dimensional Semiconductors - An Introduction* (Cambridge, 1998).
- [31] M. Nahum, T. M. Eiles, and J. M. Martinis, Appl. Phys. Lett. **65**, 3123 (1994).
- [32] M. M. Leivo, J. P. Pekola, and D. V. Averin, Appl. Phys. Lett. **52**, 5714 (1996).
- [33] A. J. Manninen, M. M. Leivo, and J. P. Pekola, Appl. Phys. Lett. **70**, 1885 (1997).
- [34] H. L. Edwards, Q. Niu, G. A. Georgakis, and A. L. de Lozanne, Phys. Rev. B **52**, 5714 (1995).
- [35] T. E. Humphrey, R. Newbury, R. P. Taylor, and H. Linke, Phys. Rev. Lett. **89**, 116801 (2002).
- [36] M. D. Ulrich, P. A. Barnes, and C. B. Vining, J. Appl. Phys. **90**, 1625 (2001).
- [37] G. J. Snyder and T. S. Ursell, Phys. Rev. Lett. **91**, 148301 (2003).
- [38] C. Vining, in *Symposium on Thermoelectric Materials - New Directions and Approaches* (1997), p. 3.
- [39] H. B. Callen, *Thermodynamics* (Wiley, New York, 1960).
- [40] T. E. Humphrey, M. F. O’Dwyer, and H. Linke, J. Phys. D **38**, 2051 (2005).
- [41] C. J. Summers and K. F. Brennan, Appl. Phys. Lett. **48**, 806 (1986).
- [42] T. K. Gaylord and K. F. Brennan, Appl. Phys. Lett. **53**, 2047 (1988).
- [43] T. Bryllert, M. Borgstrom, L.-E. Wernersson, and L. Samuelson, Appl. Phys. Lett. **82**, 2655 (2003).
- [44] M. J. Fransen, T. L. van Rooy, and P. Kruit, Applied Surface Science **146**, 312 (1999).
- [45] K. F. Brennan and C. J. Summers, J. Appl. Phys. **61**, 614 (1987).
- [46] D. Cahill, W. Ford, K. Goodson, G. Mahan, A. Majumdar, H. Maris, R. Merlin, and S. Phillpot, Applied Physics Reviews **93**, 793 (2003).
- [47] N. W. Ashcroft and N. D. Mermin, *Solid State Physics* (Saunders College Publishing, Orlando, 1976).
- [48] Y. Lin and M. S. Dresselhaus, Phys. Rev. B **68**, 075304 (2003).
- [49] A. Shakouri, Personal Communication (2005).
- [50] G. D. Mahan and J. O. Sofo, National Academy of Sciences **93**, 7436 (1996).